IMPLEMENTATION OF MULTI-CRITERIA DECISION METHOD FOR SELECTION OF REINFORCEMENT MATERIAL IN METAL MATRIX COMPOSITES FOR STEAM TURBINE BLADE

Kale Dipak R[1], Dr. R R Arakerimath[2]

Article History: Received: 10.05.2023 **Revised:** 26.06.2023 **Accepted:** 22.07.2023

Abstract

A diverse reinforcement particle in a metal matrix composite gives the high strength and low density which encourages its use in the wide range of applications. The selection of foremost reinforcement material for a metal matrix composite is accomplished via a multi-criteria decision-making method for low pressure rotating steam turbine blade which is a critical component in the steam turbine system. Based on failure cases of the blade, the various required parameters are summarized. To overcome the difficulty of material selection against various required parameters, a multi-criteria decision-making method is used. A decision framework is suggested which divides a required parameters into strength, surface property, and vibration criteria. Especially Titanium metal matrix is appraised as a substrate material for strength criteria analysis. TOPSIS and VIKOR methods of multi-criteria decision-making analysis are applied. The rank of materials is compared and revealed that both methods give the same results for the first ten materials. The result of three criteria is analyzed and optimized reinforcement particles figured out are the B_4C followed by CNT and SiC. The effect of SiC addition to the Ti and B_4C on microstructure & hardness value is investigated. The elastic resilience is directly proportional to erosion rate which is dominant failure cause in steam turbine blade is evaluated.

Keywords: Metal matrix composites, Nanoparticles, Steam turbine blade, TOPSIS, VIKOR, Ti-alloys, multi-criteria decision-making method.

[1]Research Scholar, Mechanical Engineering, G H Raisoni College of Engineering and Management, Savitribai Phule Pune University, India.
[2]Professor and dean, Jspm Rajarshi Sahu College of Engineering, Pune India.

Email: [1]drkaero@gmail.com, [2]rrarakerimath@gmail.com

DOI: 10.31838/ecb/2023.12.6.223

1. Introduction

Titanium and its alloys are widely used in the manufacturing of low pressure (LP) steam turbine rotating blades as it has a low density and good strength. A various research showed that the reinforcement of different particles like SiC, Graphene, and B_4C, etc. into the titanium alloy enhanced the mechanical properties of the components [1] and it will be the preeminent material for LP steam turbine blades. Azevedo and Feller [2] investigated and analyzed the failure cases in the steam turbine plant, which revealed that the wear and fatigue failure in the LP steam turbine blade which claim the number of people's deaths. A failure analysis by Rivaz et al [3] stated the presence of the foreign particles in the steam created a problem of corrosion in an LP steam turbine blade which leads to fatigue failure. A case study of 110 MW power plant LP steam turbine blade failure investigation carried by Cano et al [4] concluded that the crack is initiated in the blade due to centrifugal forces. Resonance fatigue analysis carried by Rodriguez et al [5] for the LP stage blade indicates that the crack initiation in the blade due to the vibrations reduces the stiffness of the blade. A review work carried by Kale & Arakerimath [6] for LP steam turbine blade failure cases summarized that the major causes of the last stage LP steam turbine blade failure are corrosion, wear, vibration, and fatigue. Now, on the other side, the metal matrix composite particularly Ti alloy as substrate with various reinforcements shows greater mechanical properties and can be the foremost material for the steam turbine blade. The addition of 0.5 wt.% graphene particles in Titanium increases the tensile strength and indicates a good balance between strength and ductility which is an important aspect [7]. Li et al [8] studied a structure using carbon nanotubes (CNT) and Ti-6Al-4V as substrate material forms an interfacial and intergranular reinforcement. The yield strength and coefficient of friction, enhanced due to the addition & uniform distributions of CNTs. Famoyi et al [9] stated that a reinforcement of composite $Zn\text{-}TiO_2/ZnTiB_2$ coating layer on mild steel components increased the service life and the anticorrosive & wear properties showed the remarkable improvement. An experiment carried by Kanyane et al [10] revealed a coating mixture of Ni and Ti powder, spread using a robot gives an excellent corrosion properties in 0.5 M H_2SO_4 solution. Arena et al [11] obtained the enhanced oxidation resistance by heating TiC+SiC composite at 500 ^oC and confirmed that the pure SiC sample is unoxidized & high oxidation is observed for pure TiC specimens. Xie et al [12] studied an addition of TiB + TiC particles in the Ti matrix shows the downside effect on rolling contact fatigue strength which happened due to stress concentration around reinforcement flakes. Madeira et al [13] revealed that the addition of SiC particles in a metal matrix composite increased the damping capacity and Young Modulus. A TOPSIS tool of multi-criteria decision method (MCDM) is an excellent tool for the selection of suitable materials for wind turbine blades considering the analytical hierarchy process for weight selection [14]. An MCDM approach is used by Caliskan et al [15] to select materials for tool holder considering various parameters. The LP stage steam turbine blade failure case studies and mechanical strength enhancement, corrosion, wear & damping property improvements are highlighted in surpassing literature and intimate the possibilities of correlativity between them for aforesaid application. The above literature revealed several varieties of reinforcement particles with wide

percentages and various manufacturing parameters are used to improve strength, corrosion & Wear, the fatigue life of the structure.

In the present work MCDM technique is used for the primary selection of reinforcement materials in metal matrix composite considered for LP steam turbine blade application. The selection of the optimized material for the applications where several parameters are required is crucial work. The result obtained in this research work gives some of the basic selection idea of reinforcement material for LP steam turbine blade as the tests carried in the literature referred are mostly not performed in the high-temperature conditions. In this work, the decision framework is developed, and using TOPSIS & VIKOR methods of MCDM the optimized reinforcement materials are obtained. The results are applicable to other applications where the same material parameters are required like gas turbine blade etc.

2. Problem statement

A steam turbine extracts the thermal energy from pressurized steam and converts it into mechanical energy in terms of the shaft rotation which is used for power generation. In the LP stage steam turbine blade due to the phase transition of the steam & the large size of the blade, the failure chances because of corrosion, wear, vibrations and centrifugal forces as shown in Fig 1 are high which makes it a critical part. The blade is subjected to the temperature, pressure and speed around 400 ^{0} C, 10 bar, 4000rpm respectively. To meet the above requirement, the properties are categorized into four criteria i.e. strength, vibration, fatigue, and surface property criteria. The metal matrix composite with various percentage contributions & type of reinforcement gives the above required properties.

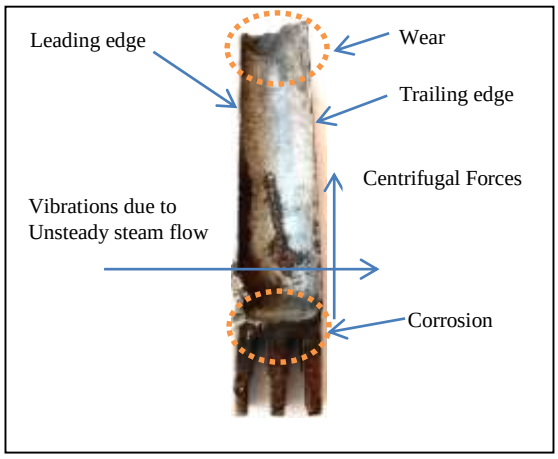

Fig. 1 The damaged steam turbine blade

None of the research work suggests the optimized reinforcement materials for the metal matrix composites which accomplished all the above demanded properties for the LP steam turbine blade. To find out the best reinforcement material, a decision framework is developed that uses a TOPSIS & VIKOR methods of MCDM. An analytical hierarchy process method is used for the selection of weight.

3. The hierarchy for a decision framework

A decision framework shows a path to get the best combination of reinforcement for metal matrix composites with the substrate preferable as Titanium alloy to achieve

required mechanical properties for the LP steam turbine blade.

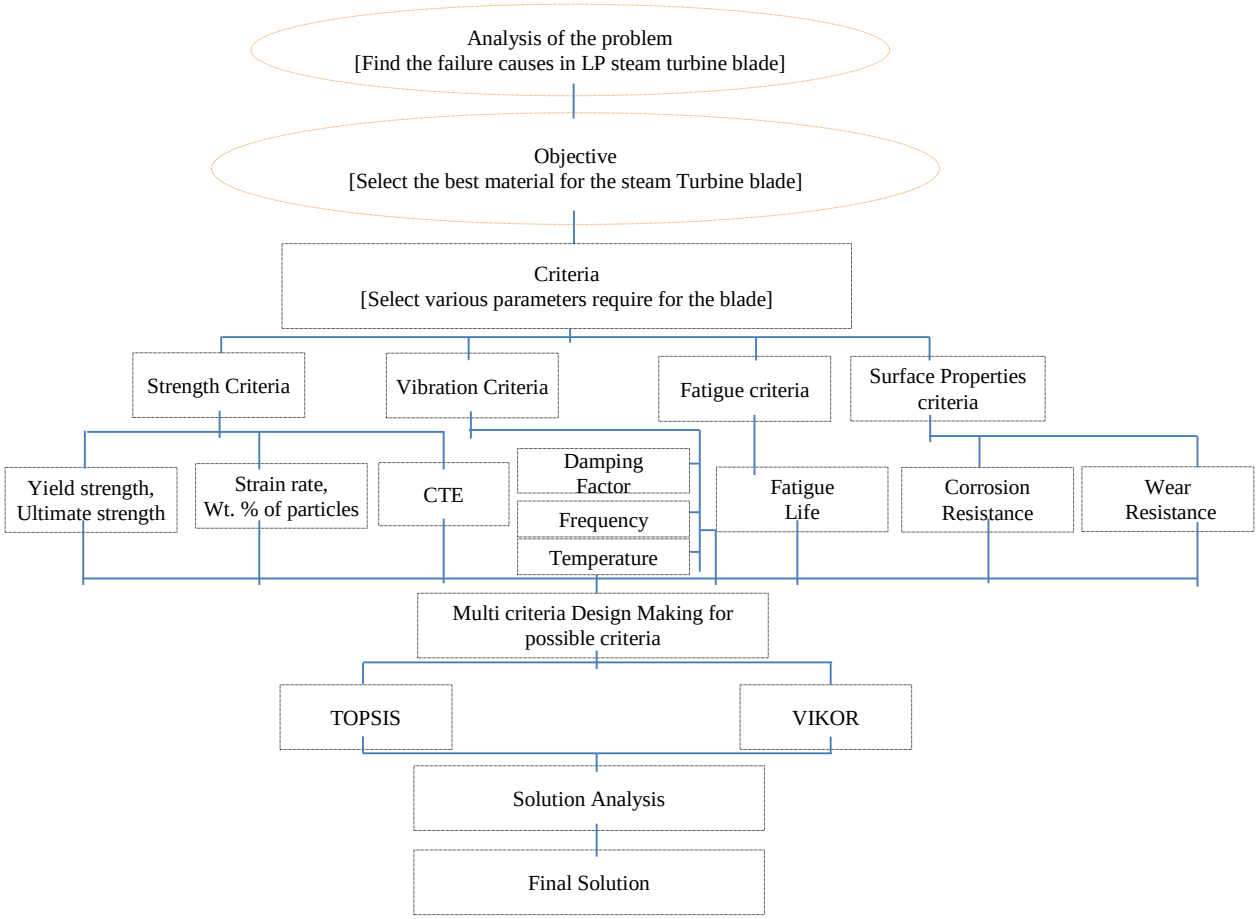

Fig. 2 A Decision framework

A decision framework consists of six steps, i.e., i) Analysis of the problems ii) Objective iii) Criteria iv) MCDM v) Solution analysis vi) Final decision. The schematic diagram of the decision framework is shown in Fig.2. As per the decision framework, in the first step, an analysis of failure causes for the steam turbine blade is carried out. The research papers [16]–[21] and literature stated in the introduction clears that the consciousness is required on the LP steam turbine rotating blade failure. In the second step based on the problem statement the objective is required to define. Through the design and material changes the required properties stated in the problem statement can be achieved. Material changes are less focused areas compared to design changes in the steam turbine blade. The metal matrix composites reinforced with various micro particles and nanoparticles enhanced the mechanical properties of the structures, which encouraged its use in the turbine blade. Considering failure cases in a third step, a various criteria are finalized i.e., Strength, vibration, fatigue, and surface properties. As per fourth step these main criteria are divided into various sub-criteria. The Strength criteria comprise the yield strength, ultimate strength, the weight percentage of the reinforcement particles, strain rate, and coefficient of thermal expansion (CTE). The yield strength is proportional to the elastic modulus and strain rate is proportional to the toughness or ductility of the material. A large difference between CTE of the substrate and reinforcement material causes the

stress concentrations which effect on the strength of the structure. The weight percentage (wt. %) of the particle is critical as the centrifugal forces will be reduced due to less density of the reinforcement particles. In the vibration criteria, damping factor along with test frequency and the temperature is appraised as all are important in the turbine blade. For fatigue sub-criteria, the fatigue life is considered as a blade always designed for infinite fatigue life. In the surface properties according to the various failure case studies, corrosion resistance and wear resistance are considered. Various researchers are working on the numbers of combinations of different particles; its percentage is studied for various mechanical properties. In the fifth step, the TOPSIS and VIKOR tools of the multi-criteria decision method is used for an optimum solution. The shortage of the research material available in the fatigue life criteria is impotent the use of multi-criteria decision-making method for it. Based on the MCDM and final solution analysis, the optimized material is selected.

4. Strength criteria analysis

In the strength criteria, strength-related parameters of the material are considered as yield stress, ultimate stress, and strain percentage. For material strength, a percentage of the reinforcement material addition plays a vital role. A considerable difference in CTE value of substrate and reinforcement material is a cause for stress concentration in the high-temperature environment.

4.1 TOPSIS method

A TOPSIS method is the simple, fast, and systematic multi-criteria decision-making method [22]. Using the Analytical Hierarchy Process, the weight for each criterion is obtained. The following steps are used in the TOPSIS method.

Step1: Create a normalized distribution matrix using Eq. (1) for various parameters of strength criteria.

$$A_{ij} = a_{ij} / \sqrt{\sum_{j}^{n} (a_{ij})^2} \qquad (1)$$

$i = 1, 2, ...n \,\&\, j = 1, 2, ...n'$ Where n is the number of options and n' is the number of sub-criteria.

Step2: Develop weighted normalized matrix by multiplying the normalized matrix by weight of each sub-criteria.

$$N_{ij} = A_{ij}.w_j \qquad (2)$$

Step 3: Locate the positive (N_j^+) & negative (N_j^-) ideal value from the weighted normalized decision matrix.

Step 4: calculate the Euclidean distance best (E_d^+) and Euclidean distance worst (E_d^-) values using Eq. (3) & (4)

$$E_d^+ = [\sum_{j}^{n} (N_{ij} - N_j^+)^2]^{0.5} \qquad (3)$$

$$E_d^- = [\sum_{j}^{n} (N_{ij} - N_j^-)^2]^{0.5} \qquad (4)$$

Step 5: Calculate the performance score value using Eq. (5) and accordingly prepare the ranking for available materials.

$$P_s = E_d^- / (E_d^+ + E_d^-) \qquad (5)$$

A developed pairwise comparison matrix is shown in Table 1. The relative ranking scale developed by Satty [23] is applied, which shows the relative importance of parameters to each other.

Table 1 Pairwise comparison matrix for the strength criteria

Criteria	wt. % of particles(C_1)	Yield stress (C_2)	Ultimate stress (C_3)	Strain percentage(C_4)	CTE(C_5)

wt. % of particles (C_1)	1.00	5.00	5.00	3.00	3.00
Yield stress (Mpa) (C_2)	0.20	1.00	3.00	3.00	3.00
Ultimate stress (Mpa) (C_3)	0.20	0.33	1.00	3.00	3.00
Strain percentage(C_4)	0.33	0.33	0.33	1.00	3.00
CTE(C_5)	0.33	0.33	0.33	0.33	1.00
Total	2.0667	7.0000	9.6667	10.3333	13.0000

The speed of the steam turbine blade is in the range of 3000rpm to 4000rpm and at this high rpm, a 1gm of mass can create a large amount of centrifugal force. In line with this, the relative scales for wt. % of the particles are given strong importance compared to yield strength and ultimate strength. Moderate importance is given to the strain percentage as it is inclined towards the ductility of the structure and subsequently, ductility relates to the toughness. Likewise, moderate importance is given to CTE as it is related to stress concentration at high temperature conditions.

The normalization of the pairwise comparison matrix is done using Eq. (1) and shown in Table 2.

Table 2 Normalized pairwise comparison matrix for the strength criteria

Criteria	C_1	C_2	C_3	C_4	C_5
C_1	0.4839	0.7143	0.5172	0.2903	0.2308
C_2	0.0968	0.1429	0.3103	0.2903	0.2308
C_3	0.0968	0.0476	0.1034	0.2903	0.2308
C_4	0.1613	0.0476	0.0345	0.0968	0.2308
C_5	0.1613	0.0476	0.0345	0.0323	0.0769
Total	1	1	1	1	1

From the normalized pairwise comparison matrix, the weight for each sub-criteria is obtained and shown in Table 3.

Table 3 Weight matrix for the strength criteria

Criteria	C_1	C_2	C_3	C_4	C_5
Weight	0.4473	0.2142	0.1538	0.1142	0.0705

From Table 3 it's clear that the weight to the particle percentage is high compared to others. As reinforcement particles have higher strength compared to substrate i.e. the overall composite yield strength and ultimate strength will be enhanced. For the LP steam turbine blade, the temperature range is from 250 ^oC to 400 ^oC and at this temperature, the changes in CTE are not high so quite low weight is assigned to the CTE parameter. The weighted normalized decision matrix is developed using step 1 and step 2 of TOPSIS analysis and shown in Table 4. The detailed parameter values are given in Table 18 of *appendix*. The volume percentage of the reinforcement

particle is converted into a weight percentage using Eq. (6).

Wt. % of particles = $(V_p \cdot \rho_p)/ (Vp \cdot \rho_p + V_s \cdot \rho_s)$ (6)

Where V_p= Volume of particles, ρ_p= density of particle material, V_s= Volume of substrate material, ρ_s = density of substrate material.

Table 4 Weighted normalized decision matrix for the strength criteria

M/C	C_1	C_2	C_3	C_4	C_5	M/C	C_1	C_2	C_3	C_4	C_5
M1	0.0000	0.0322	0.0219	0.0179	0.0000	M24	0.0000	0.0342	0.0236	0.0149	0.0000
M2	0.0041	0.0354	0.0239	0.0138	0.0173	M25	0.1412	0.0393	0.0266	0.0004	0.0028
M3	0.0081	0.0354	0.0232	0.0059	0.0173	M26	0.0000	0.0321	0.0233	0.0130	0.0000
M4	0.0122	0.0336	0.0221	0.0050	0.0173	M27	0.0081	0.0385	0.0262	0.0128	0.0161
M5	0.0000	0.0289	0.0220	0.0214	0.0000	M28	0.0000	0.0152	0.0123	0.0431	0.0000
M6	0.0024	0.0315	0.0238	0.0041	0.0173	M29	0.0049	0.0163	0.0135	0.0333	0.0161
M7	0.0024	0.0339	0.0235	0.0074	0.0173	M30	0.0098	0.0155	0.0132	0.0315	0.0161
M8	0.0024	0.0355	0.0242	0.0025	0.0173	M31	0.0147	0.0158	0.0134	0.0277	0.0161
M9	0.0000	0.0347	0.0264	0.0105	0.0000	M32	0.0000	0.0310	0.0233	0.0179	0.0000
M10	0.0024	0.0396	0.0293	0.0095	0.0173	M33	0.0231	0.0403	0.0293	0.0132	0.0073
M11	0.0024	0.0409	0.0295	0.0096	0.0173	M34	0.0462	0.0435	0.0313	0.0084	0.0073
M12	0.0024	0.0432	0.0314	0.0112	0.0173	M35	0.0000	0.0290	0.0230	0.0112	0.0000
M13	0.0000	0.0214	0.0160	0.0336	0.0000	M36	0.0529	0.0351	0.0265	0.0044	0.0019
M14	0.0008	0.0348	0.0244	0.0240	0.0173	M37	0.0622	0.0339	0.0255	0.0029	0.0022
M15	0.0016	0.0315	0.0227	0.0276	0.0173	M38	0.1151	0.0396	0.0292	0.0069	0.0020
M16	0.0049	0.0286	0.0203	0.0296	0.0173	M39	0.0000	0.0173	0.0125	0.0276	0.0000
M17	0.0130	0.0438	0.0310	0.0044	0.0136	M40	0.0041	0.0210	0.0165	0.0165	0.0063
M18	0.0000	0.0364	0.0267	0.0058	0.0000	M41	0.0081	0.0251	0.0180	0.0103	0.0063
M19	0.0073	0.0387	0.0283	0.0030	0.0028	M42	0.0122	0.0228	0.0163	0.0069	0.0063
M2	0.224	0.032	0.023	0.008	0.002	M4	0.016	0.020	0.015	0.004	0.006

0	7	1	5	3	8	3	3	8	1	1	3
M21	0.0000	0.0196	0.0145	0.0262	0.0000	M44	0.0000	0.0479	0.0336	0.0103	0.0000
M22	0.1765	0.0196	0.0142	0.0034	0.0016	M45	0.0238	0.0558	0.0373	0.0083	0.0077
M23	0.3530	0.0194	0.0146	0.0021	0.0016						

The ideal best value describes the maximum value for the parameters C_1 to C_4 as they require maximum value and the ideal worst value is the maximum value for the parameter C_5. The required ideal best values and ideal minimum values are taken from Table 4 and shown in Table 5.

Table 5 Ideal best and worst values for the strength criteria

Parameters	C_1	C_2	C_3	C_4	C_5
Max	0.3530	0.0558	0.0373	0.0431	0.0000
Min	0.0000	0.0152	0.0123	0.0004	0.0173

The Euclidean distance for the ideal best and ideal worst is calculated using Eq. (3) & (4) and shown in Table 6. The performance score P_s is calculated using Eq. (5).

Table 6 Euclidean distance and Performance score values for the strength criteria

M/C	E_d^+	E_d^-	P_s	M/C	E_d^+	E_d^-	P_s
M1	0.3550	0.0314	0.0812	M24	0.3550	0.0316	0.0817
M2	0.3514	0.0272	0.0719	M25	0.2170	0.1446	0.3999
M3	0.3482	0.0250	0.0669	M26	0.3553	0.0293	0.0763
M4	0.3444	0.0246	0.0667	M27	0.3472	0.0309	0.0818
M5	0.3550	0.0319	0.0826	M28	0.3562	0.0461	0.1145
M6	0.3542	0.0205	0.0546	M29	0.3516	0.0333	0.0866
M7	0.3537	0.0230	0.0611	M30	0.3470	0.0327	0.0860
M8	0.3541	0.0238	0.0629	M31	0.3423	0.0310	0.0831
M9	0.3553	0.0313	0.0809	M32	0.3550	0.0313	0.0809
M10	0.3530	0.0312	0.0811	M33	0.3318	0.0415	0.1111
M11	0.3530	0.0324	0.0841	M34	0.3091	0.0589	0.1600
M12	0.3527	0.0357	0.0918	M35	0.3557	0.0268	0.0701
M13	0.3554	0.0381	0.0969	M36	0.3035	0.0604	0.1660
M14	0.3540	0.0330	0.0853	M37	0.2946	0.0680	0.1876
M15	0.3533	0.0334	0.0863	M38	0.2413	0.1200	0.3322
M16	0.3503	0.0335	0.0873	M39	0.3563	0.0322	0.0830
M17	0.3427	0.0370	0.0975	M40	0.3523	0.0211	0.0566
M18	0.3556	0.0313	0.0810	M41	0.3484	0.0203	0.0552
M19	0.3485	0.0329	0.0862	M42	0.3450	0.0196	0.0537

M20	0.1358	0.2262	0.6249	M43	0.3415	0.0209	0.0577
M21	0.3560	0.0314	0.0811	M44	0.3546	0.0438	0.1100
M22	0.1859	0.1773	0.4881	M45	0.3311	0.0547	0.1418
M23	0.0594	0.3534	0.8561				

The highest P_s value shows the respective rank for various sub-criteria. The M23 material, i.e. Ti-20 vol. % TiC is the high score and first choice material.

4.2 VIKOR Method

VIKOR is a popular method to solve multi-criteria decision-making problems using index values. The simplified value $a_{ij}^{'}$ is calculated from Eq. (7) using various materials listed in Table 18 given in the *Appendix*. The normalized value $a_{ij}^{''}$ matrix is developed using the Eq. (8). The average weighted deviation (D_i), the maximum of weighted deviation (B_i), and the performance score value (P_i) is calculated using Eq. (9), Eq. (10), and Eq. (11) respectively, and all values are summarized in Table 7. υ is the weight of the strategy, the value ranges from 0 to 1 and usually taken as 0.5. The low value of P_i indicates the best material options considering all parameters with the assigned weightage.

$$a_{ij}^{'} = a_{ij} - (a_{ij})_{\min} \tag{7}$$

$$a_{ij}^{''} = a_{ij}^{'} / (a_{ij}^{'})_{\max} \tag{8}$$

$$D_i = \sum_{j=1}^{n} w_j [(a_{ij}^{''})_{\max} - a_{ij}^{''}] / [(a_{ij}^{''})_{\max} - (a_{ij}^{''})_{\min}] \tag{9}$$

$$B_i = Max\{w_j [(a_{ij}^{''})_{\max} - a_{ij}^{''}] / [(a_{ij}^{''})_{\max} - (a_{ij}^{''})_{\min}]\} \tag{10}$$

$$P_i = \upsilon[(D_i - (D_i)_{\min}) / ((D_i)_{\max} - (D_i)_{\min})] + (1-\upsilon)[(B_i - (B_i)_{\min}) / ((B_i)_{\max} - (B_i)_{\min})] \tag{11}$$

Table 7 VIKOR method analysis matrix for the strength criteria

M/C	D_i	B_i	P_i	M/C	D_i	B_i	P_i
M1	0.7344	0.4473	0.8215	M24	0.7209	0.4473	0.8063
M2	0.7808	0.4421	0.8644	M25	0.5473	0.2684	0.2975
M3	0.8013	0.4370	0.8783	M26	0.7395	0.4473	0.8271
M4	0.8151	0.4318	0.8848	M27	0.7435	0.4370	0.8135
M5	0.7414	0.4473	0.8292	M28	0.8153	0.4473	0.9121
M6	0.8301	0.4442	0.9233	M29	0.8875	0.4411	0.9823
M7	0.8108	0.4442	0.9016	M30	0.8924	0.4349	0.9768
M8	0.8109	0.4442	0.9017	M31	0.8937	0.4287	0.9674
M9	0.7134	0.4473	0.7979	M32	0.7313	0.4473	0.8180
M10	0.7398	0.4442	0.8220	M33	0.6586	0.4180	0.6849
M11	0.7307	0.4442	0.8118	M34	0.6130	0.3887	0.5825

M12	0.7030	0.4442	0.7808	M35	0.7620	0.4473	0.8524
M13	0.7850	0.4473	0.8782	M36	0.6676	0.3802	0.6287
M14	0.7580	0.4463	0.8461	M37	0.6731	0.3685	0.6143
M15	0.7754	0.4452	0.8638	M38	0.5422	0.3014	0.3497
M16	0.7956	0.4411	0.8792	M39	0.8447	0.4473	0.9451
M17	0.6917	0.4308	0.7445	M40	0.8507	0.4421	0.9428
M18	0.7153	0.4473	0.8000	M41	0.8316	0.4370	0.9124
M19	0.7024	0.4380	0.7692	M42	0.8582	0.4318	0.9330
M20	0.4774	0.1626	0.0333	M43	0.8781	0.4267	0.9464
M21	0.8240	0.4473	0.9219	M44	0.5995	0.4473	0.6702
M22	0.6690	0.2236	0.3553	M45	0.5418	0.4172	0.5526
M23	0.4477	0.1919	0.0516				

The lowest value of P_i is 0.0333 for material M20 i.e., Ti6Al4V/TiC 2 which is the best material considering all sub-criteria under the strength criteria.

4.3 Comparison of TOPSIS and VIKOR analysis

Fig.3 shows the ranking comparison between TOPSIS and VIKOR analysis for the strength criteria. The difference between material rankings of two methods is less, except for the material M28 to M31. Although only the top 10 material options are considered in all criteria selection process and the difference between rankings given by two methods is very less for these materials i.e., the first 10 materials are the same.

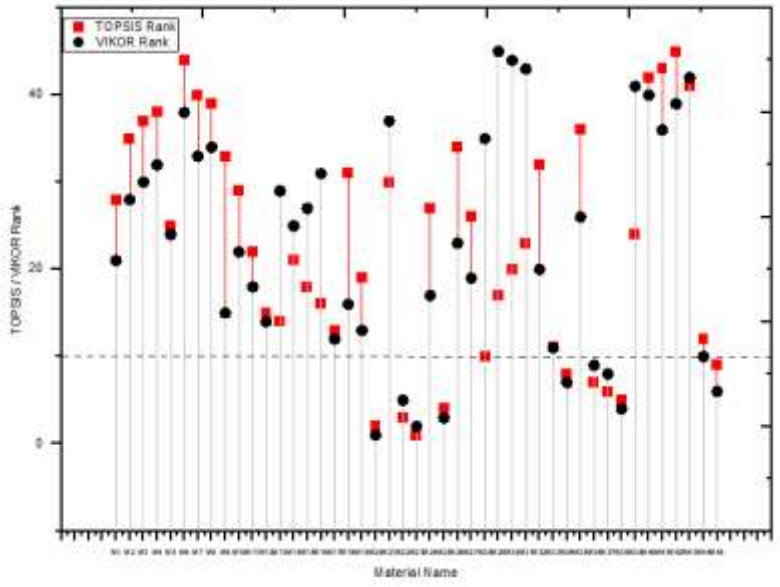

Fig. 3 TOPSIS & VIKOR rank Comparison for the strength criteria

5. Surface properties criteria analysis

The surface properties are important in the case of LP steam turbine blades as various failure case studies indicate that the blade failure occurred due to corrosion and wear problems. The various high corrosive and wear resistance materials are listed in Table 19 of Appendix which is used for optimization. The reduction in the

corrosion & wear properties are considered and calculated using Eq. (12). Both the TOPSIS & VIKOR methods are used for the best material selections.

Reduction in properties
$= (M_{bp} - M_{cp})/ M_{bp}$ (12)

Where M_{bp} is the corrosion or wear value of base material and M_{cp} is the corrosion or wear value of modified material.

5.1 TOPSIS method

The failure case studies [3], [16], [17], [19], [24]–[26]carried out for the LP steam turbine blade revealed that the failure is due to the corrosion which is the dominant and leads to wear failure. In line with this, the corrosion resistance parameter gives moderate importance compared to wear resistance parameter as shown in Table 8. The weight for corrosion resistance and wear resistance is obtained and shown in Table 9.

Table 8 Pairwise comparison matrix for the Surface properties criteria

Criteria	Corrosion Resistance	Wear Resistance
Corrosion Resistance	1.0000	3.0000
Wear Resistance	0.3333	1.0000

Table 9 Weight matrix for the Surface properties criteria

Criteria	Corrosion Resistance	Wear Resistance
Corrosion Resistance	0.75	0.75
Wear Resistance	0.25	0.25
Weight	0.75	0.25

The weighted normalized decision matrix is developed using Eq. (1) and Eq. (2) and shown in Table 10.

Table 10 Weighted normalized decision matrix for the Surface properties criteria

M/C	Corrosion Resistance	Wear Resistance	M/C	Corrosion Resistance	Wear Resistance
Mc1	0.0328	0.1932	Mc16	0.1566	0.0714
Mc2	0.0070	0.0313	Mc17	0.1508	0.0762
Mc3	0.0253	0.0313	Mc18	0.1855	0.0833
Mc4	0.0644	0.0972	Mc19	0.1744	0.2394
Mc5	0.1426	0.1389	Mc20	0.1661	0.2451
Mc6	0.1518	0.1528	Mc21	0.1690	0.2465
Mc7	0.1679	0.1944	Mc22	0.1862	0.2328
Mc8	0.1817	0.2083	Mc23	0.1869	0.2476
Mc9	-0.0121	0.1786	Mc24	0.1067	0.0543
Mc10	-0.1233	0.2321	Mc25	0.1817	0.0918
Mc11	0.1451	0.2321	Mc26	0.1832	0.1021
Mc12	0.0870	0.2321	Mc27	0.1838	0.1217
Mc13	0.0556	0.2321	Mc28	0.0758	0.0167
Mc14	0.0489	0.0418	Mc29	0.1343	0.0884

Mc15	-0.0516	0.0850	Mc30	0.1630	0.1137

The best ideal value and the worst ideal value is taken from Table 10 and shown in Table 11

Table 11 Ideal best and worst values for the Surface properties criteria

V+	0.1869	0.2476
V-	-0.1233	0.0167

The Euclidean distance ideal best (E_d^+), ideal worst (E_d^-), and the performance score (P_s) matrix are developed using Eq. (3) and Eq. (4) and shown in Table 12.

Table 12 Euclidean distance ideal best, worst and performance score matrix for the Surface properties criteria

M/C	E_d^+	E_d^-	P_s	M/C	E_d^+	E_d^-	P_s
Mc1	0.1634	0.2356	0.5905	Mc16	0.1788	0.2852	0.6147
Mc2	0.2814	0.1311	0.3179	Mc17	0.1752	0.2805	0.6155
Mc3	0.2701	0.1493	0.3560	Mc18	0.1643	0.3159	0.6579
Mc4	0.1940	0.2043	0.5129	Mc19	0.0149	0.3718	0.9615
Mc5	0.1174	0.2926	0.7137	Mc20	0.0209	0.3687	0.9464
Mc6	0.1011	0.3069	0.7522	Mc21	0.0180	0.3718	0.9539
Mc7	0.0565	0.3412	0.8580	Mc22	0.0149	0.3774	0.9621
Mc8	0.0396	0.3602	0.9009	Mc23	0.0000	0.3867	1.0000
Mc9	0.2106	0.1964	0.4826	Mc24	0.2093	0.2330	0.5268
Mc10	0.3106	0.2155	0.4096	Mc25	0.1559	0.3141	0.6683
Mc11	0.0446	0.3442	0.8853	Mc26	0.1456	0.3182	0.6861
Mc12	0.1010	0.3011	0.7488	Mc27	0.1259	0.3246	0.7205
Mc13	0.1322	0.2801	0.6794	Mc28	0.2563	0.1991	0.4372
Mc14	0.2478	0.1740	0.4126	Mc29	0.1677	0.2673	0.6145
Mc15	0.2886	0.0991	0.2555	Mc30	0.1360	0.3023	0.6897

The TOPSIS result shows that the material Mc23 i.e., Ni-P/1SiC is the first choice of the material.

5.2 VIKOR Method

The average weighted deviation (D_i), the maximum of weighted deviation (B_i), and performance score value (P_i) for Surface criteria are calculated using Eq. (9), Eq. (10), and Eq. (11) respectively, and summarized in Table 13.

Table 13 VIKOR Analysis result for the surface properties criteria

M/C	D_i	B_i	P_i	M/C	D_i	B_i	P_i
Mc1	0.4314	0.3725	0.5297	Mc16	0.2638	0.1907	0.2992
Mc2	0.6691	0.4349	0.7262	Mc17	0.2728	0.1856	0.3016

Mc3	0.6250	0.3908	0.6681	Mc18	0.1812	0.1778	0.2367
Mc4	0.4589	0.2961	0.4967	Mc19	0.0389	0.0301	0.0454
Mc5	0.2248	0.1177	0.2250	Mc20	0.0528	0.0501	0.0679
Mc6	0.1875	0.1027	0.1907	Mc21	0.0446	0.0433	0.0579
Mc7	0.1035	0.0576	0.1058	Mc22	0.0178	0.0161	0.0223
Mc8	0.0551	0.0425	0.0643	Mc23	0.0000	0.0000	0.0000
Mc9	0.5558	0.4811	0.6832	Mc24	0.4032	0.2093	0.4024
Mc10	0.7668	0.7500	1.0000	Mc25	0.1812	0.1687	0.2306
Mc11	0.1178	0.1011	0.1442	Mc26	0.1663	0.1576	0.2135
Mc12	0.2581	0.2414	0.3293	Mc27	0.1437	0.1363	0.1845
Mc13	0.3341	0.3174	0.4295	Mc28	0.5187	0.2687	0.5173
Mc14	0.5564	0.3336	0.5852	Mc29	0.2996	0.1724	0.3103
Mc15	0.7526	0.5765	0.8751	Mc30	0.2027	0.1449	0.2288

The minimum value of P_i indicates the best material choice i.e., Ni-P/1SiC is having the optimum corrosive and wear resistance.

5.3 Result comparison of TOPSIS and VIKOR

The comparison between the results of TOPSIS & VIKOR analysis is shown in the Fig.4. The difference between the ranks is less which indicates the excellence in the selection of the materials. The only change in one rank is observed for the first 10 materials and nearby 2 rank differences occur up to 15th rank material, which shows a good agreement of both the methods and makes it easy to select the best optimal material.

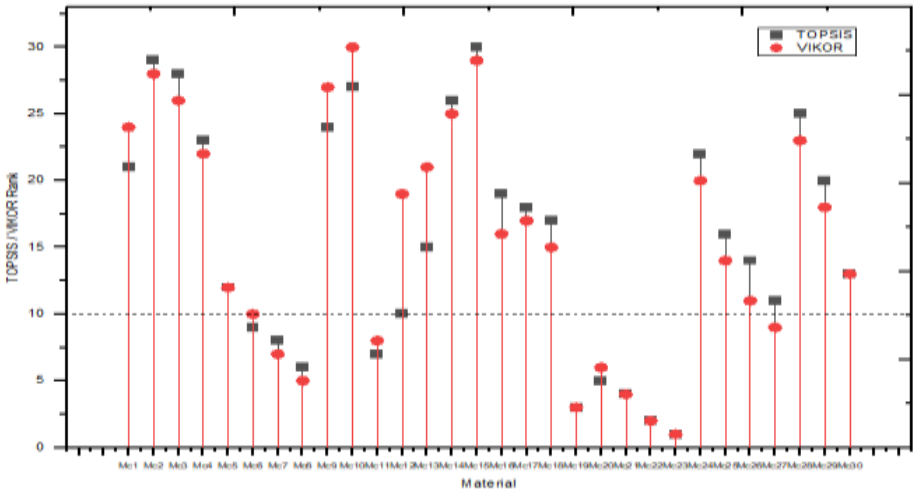

Fig. 4 TOPSIS & VIKOR rank Comparison for surface properties criteria

6. Vibration criteria

Segura et al [21] investigated that the last stage blade of the steam turbine is fractured due to high vibrations. The metallographic investigations concluded that the failure occurred due to the vibration stresses and erosion on the blades. Rodriguez et al [5] examined a low pressure stage blade at the resonance condition and it shows that the crack

initiation occurs earlier in this condition compared to normal operating condition. It indicates that the damping factor is an important parameter when selecting the material for the steam turbine blade. Rahiman & Smart [27] presented the review work summarized that the reinforcement of particles in substrate material improves the damping properties of metal matrix composites. The details of reinforcement particles are listed in Table 14 and taken from reference [28]–[35]. The values of parameters in the literature are not given specifically; to overcome this, values are considered in range and selected the lower value of that range for analysis which does not affect the performance of material for vibration criteria.

Table 14 Detail of the materials considered for the vibration criteria

Name	Reinforcement	Damping Factor	Temperature (^oC)	Frequency (Hz)	Ref.
Mp1	6 wt % sp	0.04to 0.05	250	10	[28]
Mp2	8 wt % sp	0.04to 0.05	250	10	
Mp3	6 wt % sp+2 wt % cg	0.04to 0.05	250	10	
Mp4	8 wt % sic	0.05 to 0.06	250	10	
Mp5	2 wt % CNT	0.05 to 0.06	300	50	[29]
Mp6	5 wt %SiCp	0.05 to 0.06	300	50	
Mp7	(2%+5%) wt CNT+SiCp	0.06 to 0.07	300	50	
Mp8	1 wt % CNT	0.04 to 0.05	400	30	[30]
Mp9	Carbon Fiber	0.04 to 0.05	300	1	[32]
Mp10	Cu coated Sic	0.09 to 0.12	300	4	[33]
Mp11	SiC	0.06 to 0.08	300	4	
Mp12	mg	0.06 to 0.08	300	4	
Mp13	Pure Al	0.08 to 0.09	400	1	[35]
Mp14	3wt%ofSiC	0.08 to 0.09	400	1	
Mp15	3wt%ofAl_2O_3 coated	0.09 to 0.1	400	1	
Mp16	3wt%ofZn Al_2O_3 coated	0.1 to 0.11	400	1	

The TOPSIS method is used to find the ranking of materials. From the strength and surface criteria analysis, it's clear that a TOPSIS & VIKOR method, gives the same result. Moderate importance is assigned to the damping factor and developed a pairwise comparative matrix as shown in Table 15.

Table 15 Pairwise comparative and weight matrix for the vibration criteria

Criteria	Damping Factor	Temp	frequency	Weight
Damping Factor	1.0000	3.0000	3	0.5736
Temp	0.3333	1.0000	3	0.2864
frequency	0.3333	0.3333	1	0.1399

All the steps of the TOSIS analysis method are followed, but not shown here due to space limitations. The final matrix which gives the ideal best, ideal worst and

performance score values are shown in Table16.

Table 16 TOPSIS analysis result for the vibration criteria

Reinforcement	E_d^+	E_d^-	P_s	Reinforcement	E_d^+	E_d^-	P_s
Mp1	0.1509	0.0134	0.0815	Mp9	0.1547	0.0110	0.0667
Mp2	0.1509	0.0134	0.0815	Mp10	0.0753	0.1129	0.5998
Mp3	0.1509	0.0134	0.0815	Mp11	0.1150	0.0465	0.2877
Mp4	0.1313	0.0261	0.1660	Mp12	0.1150	0.0465	0.2877
Mp5	0.1144	0.0770	0.4025	Mp13	0.0856	0.0957	0.5279
Mp6	0.1144	0.0770	0.4025	Mp14	0.0856	0.0957	0.5279
Mp7	0.0925	0.0863	0.4827	Mp15	0.0762	0.1170	0.6055
Mp8	0.1379	0.0544	0.2828	Mp16	0.0729	0.1387	0.6556

The high-performance score is for material Mp16 which contains Zinc aluminium oxide coating. Due to the consideration of the minimum range value for these criteria parameters the additional analysis is required which supports the TOPSIS analysis. Fig.5 shows the various particle reinforcement effects on the damping factor of metal matrix composites.

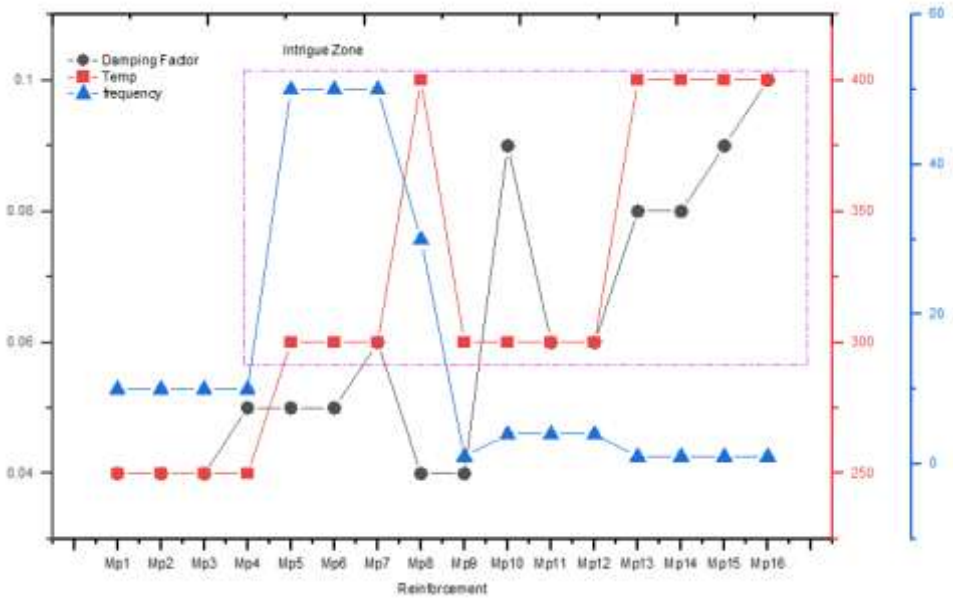

Fig.5 The Damping Factor, Temperature and Frequency value for the vibration criteria materials

The interested area, i.e., intrigue zone is highlighted using a square box based on high temperature and high damping factor requirement in the Fig.5. The material Mp7 and Mp10 to Mp16 are the best choices of materials. For material Mp13 to Mp16 the damping factor test carried out for 1Hz frequency and the same for Mp7, Mp10, Mp11 & Mp12 are conducted at a higher frequency. The damping factor depends on test frequency. From this graph and TOPSIS analysis, it's concluded that the SiC and CNT particle reinforcement is the best option for metal matrix composite.

7. Fatigue criteria

A very few research works is available in fatigue analysis of Ti alloys with reinforcement of other material particles. The CNT or MWCNT [33] shows a good fatigue strength as it bridges the crack initiation due to its excellent aspect ratio. The fatigue strength of Ti–6Al–4V with reinforcement of SiC fiber is studied by Reddy et al [34] at room temperature and indicates good results. Therefore, the fatigue criteria are not considered in MCDM analysis due to insufficient data.

8. Hardness test and SEM

A powder of Ti, B_4C and SiC has been used in current study. In Ti powder, B_4C powder is mixed (1%wt) and SiC powder with different weight percentage is mixed (1%, 3%, 5% and 7%). The powder is mixed using ball bearing milling machine with tungsten carbide balls. The specimen is prepared using spark plasma sintering powder metallurgical process at 1200^oC and 50MPa pressure. The table 17 shows Vickers micro hardness value for specimens with different compositions.

Table 17 Hardness value for different specimen

Specimen No	Composition	Hardness value
1	Ti	417
2	Ti + B_4C (1%)	513
3	Ti + B_4C (1%)+SiC(1%)	495
4	Ti+ B_4C (1%)+SiC(3%)	458
5	Ti+ B_4C (1%)+SiC(5%)	574
6	Ti+ B_4C (1%)+SiC(7%)	598

The SEM micrograph for specimen 3 and 6 are shown in Fig. 6 a and 6 b respectively.

Fig 6a SEM Micrograph for specimen 3

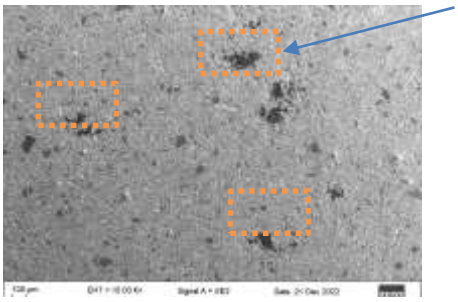

Fig 6b SEM Micrograph for specimen 6

The specimen no 6 have higher percentage of SiC which cause the accumulation of SiC. The Vickers micro hardness value for 6^{th} sample is high due to SiC higher percentage.

9. Elastic resilience for erosion rate

The elastic resilience (Ur) is directly proportional to the erosion rate due to water droplets present in the steam. The elastic resilience value for existing materials and specimen 3 material is shown in table 19 and calculated using equation 12.

$$Ur = H^2/18E \quad (12)$$

Table 18 Elastic resilience values

Sr.No.	Materials	Vickers hardness value	Elastic resilience (KPa)
1	X20Cr13	271	1889
2	X5 Base	328	2846
3	X5 laser treated	420	4667
4	Ti6Al4V	334	5634
5	Sample 3	495	11158

The elastic resilience value for sample 3 is higher than other existing materials.

10. Discussion

The contents of the top ten rank materials from all criteria are shown in Table 18.

Table 19 First ten materials from all criteria

Sr.No.	Strength Criteria	Surface Criteria	Vibration Criteria
1	20 % Vol,TiC	SiC	3wt% of ZnAl2O3 coated
2	13.8 wt % TiC	TNA10 (Ni-3Ti-B4C)	3wt% of Al2O3 coated
3	10 % Vol,TiC	TNA30(Ni-3Ti-B4C)	Cu coated SiC
4	8 % Vol,TiC	TNA20(Ni-3Ti-B4C)	3wt%ofSiC
5	4 vol.% Ti5Si3 + 3.4 vol.%TiBw	Nano-TiO2 (2.46 wt %)	(2%+5%) wt CNT+SiCp
6	4 vol.% Ti5Si3	TiSiN-2	2 wt % CNT
7	3.4 vol.% TiBw	Nano-TiO2 (1.62 wt %)	5 wt %SiCp
8	5 vol.% TiB + TiC (B_4C)	Nano-TiO2 (1.58 wt %)	SiC
9	SiC fibers 2.3 vol %	TiSiN-3	1 wt % CNT
10	2.5 vol.% TiB + TiC (B_4C)	CNT	8 wt % SiC

According to strength criteria analysis, TiC is the best choice of the material but the density of TiC is higher than the titanium material which results in high centrifugal forces and for this material, the surface and vibration criteria rank is also not available. Therefore, instead of having higher strength, TiC cannot be appropriate reinforcement material for the steam turbine blade application. The same type of reason is applicable to titanium oxide material as it has adequate corrosion and wear properties. The boron carbide particles are a good fit in strength criteria and surface criteria. The carbon nanotubes are superior in Surface and vibration criteria properties, however in strength properties analysis its received minute low rank. It indicates that the combination of CNT and B_4C particles in metal matrix composite will give better all three criteria strength. Some particles like titanium

carbide, silicon carbide, aluminum oxide, and Zinc aluminum oxide are specifically good for one criterion, and for other criteria, they are not in rank. The B_4C particles are good in all three criteria and probably the best material for the steam turbine blade application. From the above result the best three material particles suggested are Silicon carbide, Boron carbide, and Carbon nanotubes. When the sintering temperature is above 1000 ^oC for SiC reinforced titanium matrix composite, then the following reaction as shown in Eq. (13) happens and the benefit of SiC towards the whole composite will be reduced.

$$SiC + Ti = TiC+Si \quad (13)$$

The generation of Silica causes pitting and corrosion problems in LP steam turbine blades. To avoid this problem and get the benefit of SiC strength and density, it can be used inside of the blade so that it will not be in contact with steam. In strength criteria, titanium is considered as substrate material which reflects an excellent bond with the reinforcement materials. Therefore, the B_4C, SiC, and CNT are the preferred material with titanium & for other substrate materials, the investigations are needed. An erosion resistance of the blade material with steam environment depends on the hardness of the materials [36]. The Vickers hardness test result for Ti+ B_4C (1%) + SiC(7%) is higher compare to other specimens. The SEM analysis indicates that SiC is accumulated at several areas and it will have weak bond with other materials. So, hardness test and SEM analysis indicates that the Ti+ B_4C (1%) + SiC(1%) will be good choice of materials. Therefore, the aforesaid optimized reinforcement material increases the hardness and along with this, it will also improve the other required mechanical properties related to the strength and vibration criteria.

11. Conclusion

A decision framework is developed to select possible optimized reinforcement materials for metal matrix composites based on three criteria. The weight for each parameter of all criteria is found out using the analytical hierarchy process. MCDM tools, i.e., TOPSIS & VIKOR successfully applied to strength, corrosion, and vibration criteria which are considered for LP steam turbine blade applications. The best ten materials are selected for each criteria based on ranking obtained from MCDM results. In strength criteria, TiC, SiC, TiBw, and B_4C are the preferred reinforcement material particles as they have excellent yield strength, ultimate tensile strength, and strain rate. For these reinforcement materials, the CTE value is not far away from the base material value. SiC, B_4C, and CNT have excellent corrosion and wear resistance which reflects a top prioritization of them in surface criteria. The SiC and CNT materials are preferred in MCDM results due to their good damping properties in high-temperature environments. The three criteria results are compared to each other to find out the best particle reinforcement. The boron carbide & carbon nanotube particles are suggested based on three criteria for the LP steam turbine blade application & SiC is preferred with the condition that it should not be exposed to the steam. The hardness test result and elastic resilience evaluation shows the reinforcement of B_4C (1% wt) and SiC (1%wt) will be the best choice. However, a practical exposure to the standard test environment considering specimens made with the reinforcement of SiC and B_4C is required to bridge the gap between analytical and practical results.

Declaration of interests

The authors declare that they have no known competing financial interests or personal relationships that could have

appeared to influence the work reported in this paper.

Acknowledgment

The use of SPS facility at IIT Kanpur, procured with partial funding from Department of Science and Technology, Government of India as well as CARE funding from IIT Kanpur, is gratefully acknowledged. The author is grateful to Mr. Hemant Bari, a member of the condition monitoring society of India for giving valuable practical knowledge related to the failure of the steam turbine blades.

CRediT author statement

Kale Dipak R: Conceptualization, methodology, original draft preparation, R R Arakerimath: Supervision, Reviewing.

12. References

[1] M. Y. Zhou *et al.*, 'Progress in research on hybrid metal matrix composites', *J. Alloys Compd.*, vol. 838, 2020.

[2] C. R. F. Azevedo and A. H. Feller, 'Selected cases of failure analysis and the regulatory agencies in Brazil. Part 2: Electric energy and oil', *Eng. Fail. Anal.*, vol. 99, no. October 2018, pp. 108–125, 2019.

[3] A. Rivaz, S. H. Mousavi Anijdan, and M. Moazami-Goudarzi, 'Failure analysis and damage causes of a steam turbine blade of 410 martensitic stainless steel after 165,000 h of working', *Eng. Fail. Anal.*, vol. 113, p. 104557, 2020.

[4] S. Cano *et al.*, 'Detection of damage in steam turbine blades caused by low cycle and strain cycling fatigue', *Eng. Fail. Anal.*, vol. 97, no. August 2018, pp. 579–588, 2019.

[5] J. A. Rodríguez *et al.*, 'Fatigue of steam turbine blades at resonance conditions', *Eng. Fail. Anal.*, vol. 104, no. August 2018, pp. 39–46, 2019.

[6] A. R. Rajendra K.D., 'Analysis of Steam Turbine Blade Failure Causes', in *ICRRM 2019 – System Reliability, Quality Control, Safety, Maintenance and Management*, Singapore: Springer Singapore, 2020, pp. 46–52.

[7] F. Zhang, J. Wang, T. Liu, and C. Shang, 'Enhanced mechanical properties of few-layer graphene reinforced titanium alloy matrix nanocomposites with a network architecture', *Mater. Des.*, vol. 186, p. 108330, 2020.

[8] S. Li *et al.*, 'Interfacial/intragranular reinforcement of titanium-matrix composites produced by a novel process involving core-shell structured powder', *Carbon N. Y.*, vol. 164, pp. 378–390, 2020.

[9] O. S. I. Fayomi, A. P. I. Popoola, L. R. Kanyane, and T. Monyai, 'Development of reinforced in-situ anti-corrosion and wear Zn-TiO2/ZnTiB2 coatings on mild steel', *Results Phys.*, vol. 7, pp. 644–650, 2017.

[10] L. R. Kanyane, O. S. Adesina, A. P. I. Popoola, G. A. Farotade, and N. Malatji, 'Microstructural evolution and corrosion properties of laser clad Ti-Ni on titanium alloy (Ti6Al4V)', *Procedia Manuf.*, vol. 35, pp. 1267–1272, 2019.

[11] H. Aréna *et al.*, 'Effect of TiC incorporation on the optical properties and oxidation resistance of SiC ceramics', *Sol. Energy Mater. Sol. Cells*, vol. 213, no. March, 2020.

[12] L. Xie *et al.*, 'Effect of reinforcements on rolling contact fatigue behaviors of titanium matrix composite (TiB+TiC)/Ti–6Al–4V', *Int. J. Fatigue*, vol. 66, pp. 127–137, Sep. 2014.

[13] S. Madeira, G. Miranda, D. Soares, F. S. Silva, and O. Carvalho, 'Study on damping capacity and dynamic

Young's modulus of aluminium matrix composite reinforced with SiC particles', *Cienc. e Tecnol. dos Mater.*, vol. 29, no. 1, pp. e92–e96, 2017.

[14] I. P. Okokpujie, U. C. Okonkwo, C. A. Bolu, O. S. Ohunakin, M. G. Agboola, and A. A. Atayero, 'Implementation of multi-criteria decision method for selection of suitable material for development of horizontal wind turbine blade for sustainable energy generation', *Heliyon*, vol. 6, no. 1, p. e03142, 2020.

[15] H. Çalişkan, B. Kurşuncu, C. Kurbanoğlu, and şevki Y. Güven, 'Material selection for the tool holder working under hard milling conditions using different multi criteria decision making methods', *Mater. Des.*, vol. 45, pp. 473–479, 2013.

[16] D. Ziegler, M. Puccinelli, B. Bergallo, and A. Picasso, 'Investigation of turbine blade failure in a thermal power plant', *Biochem. Pharmacol.*, vol. 1, no. 3, pp. 192–199, 2013.

[17] M. C. Antony Harison, M. Swamy, A. H. V. Pavan, and G. Jayaraman, 'Root Cause Analysis of Steam Turbine Blade Failure', *Trans. Indian Inst. Met.*, vol. 69, no. 2, pp. 659–663, 2016.

[18] E. Plesiutschnig, P. Fritzl, N. Enzinger, and C. Sommitsch, 'Fracture analysis of a low pressure steam turbine blade', *Case Stud. Eng. Fail. Anal.*, vol. 5–6, pp. 39–50, 2016.

[19] L. K. Bhagi, P. Gupta, and V. Rastogi, 'Fractographic investigations of the failure of L-1 low pressure steam turbine blade', *Case Stud. Eng. Fail. Anal.*, vol. 1, no. 2, pp. 72–78, 2013.

[20] M. Nurbanasari, 'Carck of a first stage blade in a steam Turbine', *Biochem. Pharmacol.*, 2014.

[21] J. A. Segura, L. Castro, I. Rosales, J. A. Rodriguez, G. Urquiza, and J. M. Rodriguez, 'Diagnostic and failure analysis in blades of a 300 MW steam turbine', *Eng. Fail. Anal.*, vol. 82, no. July 2016, pp. 631–641, 2017.

[22] C. L. Hwang and A. S. M. Masud, 'Multiple Objective Decision Making - Methods and Applications', *Lect. Notes Econ. Math. Syst.*, vol. 1, no. 164, pp. 1–358, 1979.

[23] T. L. Saaty, 'Decision making with the analytic hierarchy process', *Int. J. Serv. Sci.*, vol. 1, no. 1, p. 83, 2008.

[24] A. D. Kushwaha, A. Soni, and L. Garewal, 'Critical Review paper of Steam Turbine Blades Corrosion and its Solutions', vol. 3, no. 4, pp. 776–784, 2014.

[25] K. L. Bhagi, V. Ratogi, and P. Gupta, 'A Brief Review on Failure of Turbine Blades', *Proc. STME-2013 Smart Technol. Mech. Eng.*, no. October, pp. 1–8, 2013.

[26] D. N. Adnyana, 'Corrosion Fatigue of a Low-Pressure Steam Turbine Blade', *J. Fail. Anal. Prev.*, 2018.

[27] A. H. S. Rahiman and D. S. R. Smart, 'Damping Characteristics of Aluminium Matrix Composites – A Review', *Mater. Today Proc.*, vol. 11, pp. 1139–1143, 2019.

[28] K. K. Alaneme and A. V. Fajemisin, 'Evaluation of the damping behaviour of Al-Mg-Si alloy based composites reinforced with steel, steel and graphite, and silicon carbide particulates', *Eng. Sci. Technol. an Int. J.*, vol. 21, no. 4, pp. 798–805, 2018.

[29] O. Carvalho, G. Miranda, M. Buciumeanu, M. Gasik, F. S. Silva, and S. Madeira, 'High temperature damping behavior and dynamic

Young's modulus of AlSi-CNT-SiCphybrid composite', *Compos. Struct.*, vol. 141, pp. 155–162, 2016.

[30] C. F. Deng, D. Z. Wang, X. X. Zhang, and Y. X. Ma, 'Damping characteristics of carbon nanotube reinforced aluminum composite', *Mater. Lett.*, vol. 61, no. 14–15, pp. 3229–3231, 2007.

[31] K. K. Deng, J. C. Li, K. B. Nie, X. J. Wang, and J. F. Fan, 'High temperature damping behavior of as-deformed Mg matrix influenced by micron and submicron SiCp', *Mater. Sci. Eng. A*, vol. 624, pp. 62–70, 2015.

[32] J. Gu, X. Zhang, M. Gu, Z. Liu, and G. Zhang, 'The damping capacity of aluminum matrix composites reinforced with coated carbon fibers', *Mater. Lett.*, vol. 58, no. 25, pp. 3170–3174, 2004.

[33] J. Gu, X. Zhang, Y. Qiu, and M. Gu, 'Damping behaviors of magnesium matrix composites reinforced with Cu-coated and uncoated SiC particulates', *Compos. Sci. Technol.*, vol. 65, no. 11–12, pp. 1736–1742, 2005.

[34] M. Penchal Reddy *et al.*, 'Enhancing compressive, tensile, thermal and damping response of pure Al using BN nanoparticles', *J. Alloys Compd.*, vol. 762, pp. 398–408, 2018.

[35] S. Singh and K. Pal, 'Effect of surface modified silicon carbide particles with Al2O3 and nanocrystalline spinel ZnAl2O4 on mechanical and damping properties of the composite', *Mater. Sci. Eng. A*, vol. 644, pp. 325–336, 2015.

[36] M. Ahmad, M. Casey, and N. Sürken, 'Experimental assessment of droplet impact erosion resistance of steam turbine blade materials', *Wear*, vol. 267, no. 9–10, pp. 1605–1618, 2009.

[37] L. L. Dong *et al.*, 'Carbonaceous nanomaterial reinforced Ti-6Al-4V matrix composites: Properties, interfacial structures and strengthening mechanisms', *Carbon N. Y.*, vol. 164, pp. 272–286, 2020.

[38] J. Lu *et al.*, 'Simultaneously enhancing the strength and ductility in titanium matrix composites via discontinuous network structure', *Compos. Part A Appl. Sci. Manuf.*, vol. 136, no. May, 2020.

[39] Y. Liu, S. Li, R. D. K. Misra, K. Geng, and Y. Yang, 'Planting carbon nanotubes within Ti-6Al-4V to make high-quality composite powders for 3D printing high-performance Ti-6Al-4V matrix composites', *Scr. Mater.*, vol. 183, pp. 6–11, 2020.

[40] H. Attar, S. Ehtemam-Haghighi, D. Kent, and M. S. Dargusch, 'Recent developments and opportunities in additive manufacturing of titanium-based matrix composites: A review', *Int. J. Mach. Tools Manuf.*, vol. 133, no. June, pp. 85–102, 2018.

[41] Z. Cao *et al.*, 'Reinforcement with graphene nanoflakes in titanium matrix composites', *J. Alloys Compd.*, vol. 696, pp. 498–502, 2017.

[42] L. L. Dong *et al.*, 'Mechanisms of simultaneously enhanced strength and ductility of titanium matrix composites reinforced with nanosheets of graphene oxides', *Ceram. Int.*, vol. 45, no. 15, pp. 19370–19379, 2019.

[43] L. Huang, L. Wang, M. Qian, and J. Zou, 'High tensile-strength and ductile titanium matrix composites strengthened by TiB nanowires', *Scr. Mater.*, vol. 141, pp. 133–137, 2017.

[44] Y. Jiao *et al.*, 'Strengthening and plasticity improvement mechanisms of titanium matrix composites with two-scale network microstructure', *Powder Technol.*, vol. 356, pp. 980–989, 2019.

[45] Y. Liu *et al.*, 'Microstructure and mechanical properties of SiC nanowires reinforced titanium matrix composites', *J. Alloys Compd.*, vol. 819, no. xxxx, p. 152953, 2020.

[46] A. Muthuchamy, G. D. J. Ram, and V. S. Sarma, 'Spark plasma consolidation of continuous fiber reinforced titanium matrix composites', *Mater. Sci. Eng. A*, vol. 703, pp. 461–469, 2017.

[47] D. Sharma, S. Mohanty, and A. K. Das, 'Surface & Coatings Technology Surface modi fi cation of titanium alloy using hBN powder mixed dielectric through micro-electric discharge machining', *Surf. Coat. Technol.*, vol. 381, no. October 2019, p. 125157, 2020.

[48] K. S. Prakash, P. M. Gopal, D. Anburose, and V. Kavimani, 'Mechanical , corrosion and wear characteristics of powder metallurgy processed Ti-6Al-4V / B 4 C metal matrix composites', *Ain Shams Eng. J.*, vol. 9, no. 4, pp. 1489–1496, 2018.

[49] C. Lee, 'Fabrication , characterization and wear corrosion testing of bioactive hydroxyapatite / nano-TiO 2 composite coatings on anodic Ti – 6Al – 4V substrate for biomedical applications', *Mater. Sci. Eng. B*, vol. 177, no. 11, pp. 810–818, 2012.

[50] F. Movassagh-alanagh, A. Abdollah-zadeh, M. Aliofkhazraei, and M. Abedi, 'Improving the wear and corrosion resistance of Ti – 6Al – 4V alloy by deposition of TiSiN nanocomposite coating with pulsed-DC PACVD', *Wear*, vol. 390–391, no. May, pp. 93–103, 2017.

[51] S. Sathish, M. Geetha, N. D. Pandey, C. Richard, and R. Asokamani, 'Studies on the corrosion and wear behavior of the laser nitrided biomedical titanium and its alloys', *Mater. Sci. Eng. C*, vol. 30, no. 3, pp. 376–382, 2010.

[52] X. He, R. G. Song, and D. J. Kong, 'E ff ects of TiC on the microstructure and properties of TiC / TiAl composite coating prepared by laser cladding', vol. 112, no. July 2018, pp. 339–348, 2019.

[53] J. Shen, B. Zou, X. Cai, S. Dong, and X. Cao, 'Fabrication and properties of TiB2-TiC reinforced NiAl coatings by reactive plasma spraying on AZ91D magnesium alloy', *Surf. Coat. Technol.*, p. 125055, 2019.

[54] N. Ghavidel, S. R. Allahkaram, R. Naderi, M. Barzegar, and H. Bakhshandeh, 'Corrosion and wear behavior of an electroless Ni-P/nano-SiC coating on AZ31 Mg alloy obtained through environmentally-friendly conversion coating', *Surf. Coatings Technol.*, vol. 382, p. 125156, Jan. 2020.

[55] C. K. Lee, 'Tribology International Wear and corrosion behavior of electrodeposited nickel – carbon nanotube composite coatings on Ti – 6Al – 4V alloy in Hanks 0 solution', *Tribiology Int.*, vol. 55, pp. 7–14, 2012.

[56] J. Lei, C. Shi, S. Zhou, Z. Gu, and L. Zhang, 'Enhanced corrosion and wear resistance properties of carbon fi ber reinforced Ni-based composite coating by laser cladding', *Surf. Coat. Technol.*, vol. 334, no. November 2017, pp. 274–285, 2018.

[57] A. Akyol, H. Algul, M. Uysal, H. Akbulut, and A. Alp, 'A Novel Approach for Wear and Corrosion Resistance in the Electroless Ni-P-W alloy with CNFs Co-Depositions', *Appl. Surf. Sci.*, 2018.

Appendix

Table 20 Detail of the materials considered for the Strength criteria.

M/C	Material Name	C_1	C_2	C_3	C_4	CTE *10^-6/k			Ref
						C_{5s}	C_{5r}	C_5	
M1	Ti6Al4V	0	853	884	13	9.2	9.2	0	[7]
M2	Ti6Al4V/Graphene	0.25	940	968	10	9.2	-2	11.2	
M3		0.5	938	940	4.3	9.2	-2	11.2	
M4		0.75	892	892	3.6	9.2	-2	11.2	
M5	SPS Ti6Al4V	0	767.5	889.9	15.5	9.2	9.2	0	[37]
M6	SPS Ti6Al4V /graphite powder	0.15	835.79	963.22	3	9.2	-2	11.2	
M7	SPS Ti6Al4V/graphene Nano plates	0.15	897.68	951.11	5.4	9.2	-2	11.2	
M8	SPS Ti6Al4V/graphene oxide Nano sheets	0.15	941.96	979.93	1.8	9.2	-2	11.2	
M9	HR Ti6Al4V	0	920	1066	7.6	9.2	9.2	0	[37]
M10	HR Ti6Al4V/graphite powder	0.15	1049.56	1183.39	6.9	9.2	-2	11.2	
M11	HR Ti6Al4V/graphene Nano plates	0.15	1085.4	1194.06	7	9.2	-2	11.2	
M12	HR Ti6Al4V/graphene oxide Nano sheets	0.15	1146.36	1269.66	8.1	9.2	-2	11.2	
M13	Ti–3Al–3Zr–1Mo/GNP 1	0	567.77	647.96	24.4	9.2	9.2	0	[38]
M14		0.05	924.17	986.42	17.4	9.2	-2	11.2	
M15		0.1	835.78	917.73	20	9.2	-2	11.2	
M16		0.3	759.51	820.97	21.5	9.2	-2	11.2	
M17	Ti6Al4V/CNT	0.8	1162	1255	3.2	9.2	0.4	8.8	[39]
M18	Ti6Al4V	0	964	1078	4.2	9.2	9.2	0	
M19	Ti6Al4V/TiC 1	0.45	1027	1143	2.2	9.2	7.4	1.8	
M20		13.8	850	950	6	9.2	7.4	1.8	
M21	CP-Ti	0	520	585	19	8.41	8.41	0	[40]
M22	Ti/TiC	10.84	520	575	2.5	8.41	7.4	1.01	
M23		21.68	515	590	1.5	8.41	7.4	1.01	
M24	Ti6Al4V	0	907	956	10.8	9.2	9.2	0	[40]
M25	Ti6Al4V/TiC	8.67	1041	1075	0.3	9.2	7.4	1.8	
M26	Ti	0	850	942	9.4	8.41	8.41	0	[41]
M27	Ti / GNFs	0.5	1021	1058	9.3	8.41	-2	10.41	
M28	Ti	0	403	497	31.3	8.41	8.41	0	[42]
M29	GONs/Ti	0.3	433	545	24.2	8.41	-2	10.41	
M30		0.6	410	534	22.9	8.41	-2	10.41	
M31		0.9	419	541	20.1	8.41	-2	10.41	
M32	Ti6Al4V	0	823	944	13	9.2	9.2	0	[43]
M33	Ti6Al4V /TiB + TiC	1.42	1070	1184	9.6	9.2	4.5	4.7	

M34	(B4C)	2.84	1153	1267	6.1	9.2	4.5	4.7	
M35	Ti	0	770	930	8.1	8.41	8.41	0	[44]
M36	Ti/TiBw	3.25	930	1070	3.2	8.41	7.2	1.21	
M37	Ti/Ti5Si3	3.82	900	1030	2.1	8.41	7	1.41	
M38	Ti/Ti5Si3 + TiBw	7.07	1050	1180	5	8.41	7.1	1.31	
M39	Ti	0	459	504	20	8.41	8.41	0	[45]
M40	Ti/ SiCNWs	0.25	556	668	12	8.41	4.3	4.11	
M41		0.5	665	726	7.5	8.41	4.3	4.11	
M42		0.75	604	658	5	8.41	4.3	4.11	
M43		1	552	609	3	8.41	4.3	4.11	
M44	Ti-15V-3Cr-3Sn-3Al	0	1270	1360	7.5	9.1	9.1	0	[46]
M45	Ti+Sic fibers	1.46	1480	1510	6	9.1	4.1	5	

Table 21 Detail of the materials considered for the Surface criteria.

M/C	Material Name	Corrosion		Wear		Ref.
		Current density/Corrosion Rate	% Increment	Wear Rate	% Increment	
Mb1	Ti6Al4V	5.92	-	0.22		[47]
Mc1	hBN powder, hexagonal boron nitride powder	4.89	0.1739	0.05	0.7727	
Mb2	Ti6Al4V	6.72		8		[48]
Mc2	5 % B4C	6.47	0.0372	7	0.125	
Mc3	10 % B4C	5.82	0.1339	7	0.125	
Mb3	Ti6Al4V	0.82		0.009		[49]
Mc4	nano-TiO2 (1.16 wt %)	0.54	0.3414	0.0055	0.3888	
Mc5	nano-TiO2 (1.23 wt %)	0.2	0.7560	0.004	0.5555	
Mc6	nano-TiO2 (1.58 wt %)	0.16	0.8048	0.0035	0.6111	
Mc7	nano-TiO2 (1.62 wt %)	0.09	0.8902	0.002	0.7777	
Mc8	nano-TiO2 (2.46 wt %)	0.03	0.9634	0.0015	0.8333	
Mb4	Ti6Al4V	1.56		3.5		[50]
Mc9	TiN	1.66	-0.0641	1	0.7142	
Mc10	TiSiN-1	2.58	-0.6538	0.25	0.9285	
Mc11	TiSiN-2	0.36	0.7692	0.25	0.9285	
Mc12	TiSiN-3	0.84	0.4615	0.25	0.9285	
Mc13	TiSiN-4	1.1	0.2948	0.25	0.9285	
Mb5	Ti	0.856		0.000004443		[51]
Mc14	C.P titanium-	0.634	0.2593	0.0000037	0.1672	

	laser nitrided					
Mc15	Ti–13Nb–13Zr-laser nitrided	1.09	-0.2733	0.000002933	0.3398	
Mb6	TiAl alloys	2.7706		105		[52]
Mc16	20% TiC (μm) A coating	0.46941	0.8305	75	0.2857	
Mc17	10% TiC (nm) B coating	0.55547	0.7995	73	0.3047	
Mc18	20% TiC (nm) C coating	0.045395	0.9836	70	0.3333	
Mb7	AZ91D	261.3		194.5		[53]
Mc19	TNA10 (Ni-3Ti-B4C)	19.6	0.9249	8.237	0.9576	
Mc20	TNA20(Ni-3Ti-B4C)	31.1	0.8809	3.804	0.9804	
Mc21	TNA30(Ni-3Ti-B4C)	27.2	0.8959	2.736	0.9859	
Mb8	AZ31mg alloy	132.1		441.1		[54]
Mc22	Ni-P	1.7	0.9871	30.4	0.9310	
Mc23	Ni-P/1SiC	1.2	0.9909	4.2	0.9904	
Mb9	Ni	0.99		2.67		[55]
Mc24	Ni-5 g/lCNT	0.43	0.5656	2.09	0.2172	
Mc25	Ni-15 g/lCNT	0.036	0.9636	1.69	0.3670	
Mc26	Ni-20 g/lCNT	0.028	0.9717	1.58	0.4082	
Mc27	Ni-30 g/lCNT	0.025	0.9747	1.37	0.4868	
Mb10	0% CF	2.35		3.75		[56]
Mc28	6 vol% CFs	1.406	0.4017	3.5	0.0666	
Mb11	Ni-P-W (60 g/L Na2WO4)	420		3.48		[57]
Mc29	Ni-P-W (100 g/L Na2WO4 and 0.1 g/L CNFs)	121	0.7119	2.25	0.3534	
Mc30	Ni-P-W (100 g/L Na2WO4 and 0.2 g/L CNFs)	57	0.8642	1.897	0.4548	